Supplemental figures:

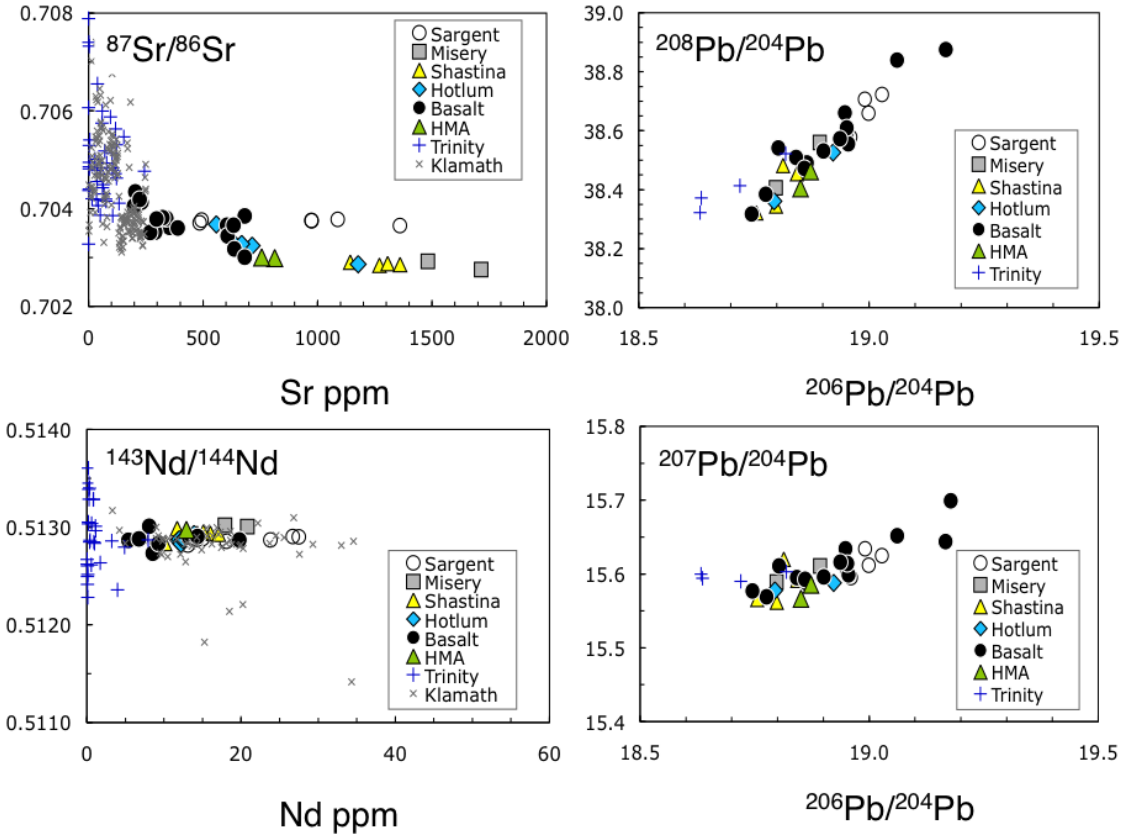

Supplemental Figure A1. This figure compares Sr, Nd, and Pb isotopic compositions of Shasta HMA (average of our data [4 samples] and analysis of sample 85-41b; cf. Table 1) with similar data for other Shasta area lavas and representative country rocks. For convenience, data for Shasta dacites (four age groups) and basalts are distinguished by different symbols. Comparative data are also shown for likely basement rocks in the vicinity of Mt. Shasta; these include ultramafic and gabbroic rocks of the Trinity Ophiolite and a variety of generally granitoid rocks from nearby Klamath Mtn. tectonic terranes.

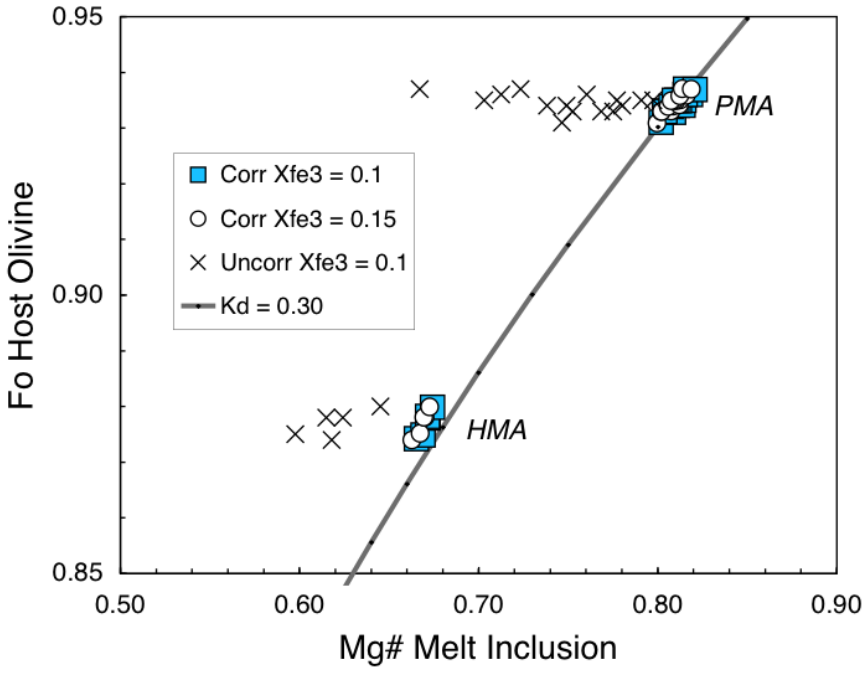

SUPPLEMENTAL FIGURE A2. Mg# and host olivine Fo mole fraction for melt inclusions (MIs) from the Whaleback HMA (data from Ruscitto et al., 2011). 'Uncorrected' MI compositions display highly variable Mg#. After PEC correction, MIs of HMA and PBA bulk compositions cluster near the loci for olivine-melt Fe-Mg equilibrium for olivine and coexisting melt, corresponding to their distinct host olivine compositions.

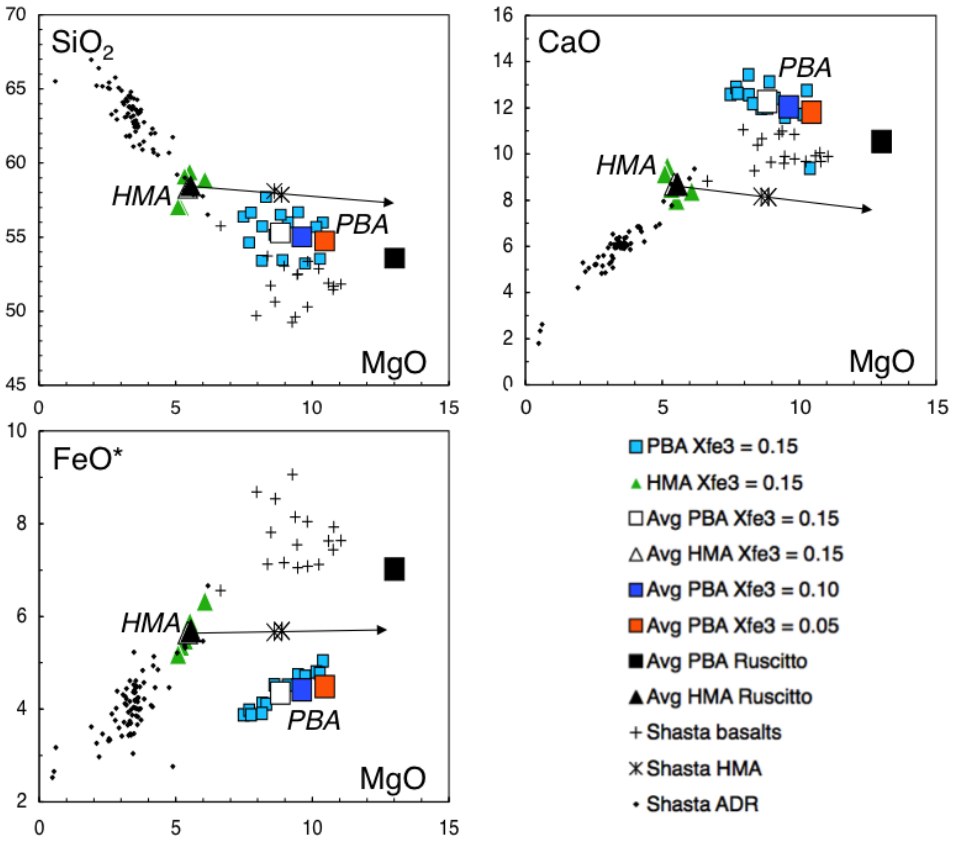

SUPPLEMENTAL FIGURE A3. Selected major element variations in HMA (triangles) and PBA (squares) melt inclusions (MIs). Large symbols represent averages. For HMA our average (open triangle) overlaps the average of Ruscitto et al. (black triangle). For PBA our averages (calculated for X-fe3 ranging from 0.05 to 0.15, and distinguished by color) are significantly lower in MgO and FeO* compared to the Ruscitto et al. estimates. To illustrate the heterogeneity of the respective MI groups, individual MIs are plotted for X-fe3 = 0.15. Also, for comparison we show whole rock analyses for Shasta basalts, high-Mg andesites (HMA), and andesite-dacite-rhyolite (ADR) lavas. Note that HMA MIs lie on near-linear arrays between Shasta basalts and ADR lavas in all plots, consistent with a mixing origin for the HMA liquids. HMA bulk rock compositions are displaced from such arrays; relative to the HMA MIs they lie on vectors consistent with addition of material (with similar FeO*, lower CaO, and higher MgO) distinct from all Shasta lavas or MIs.

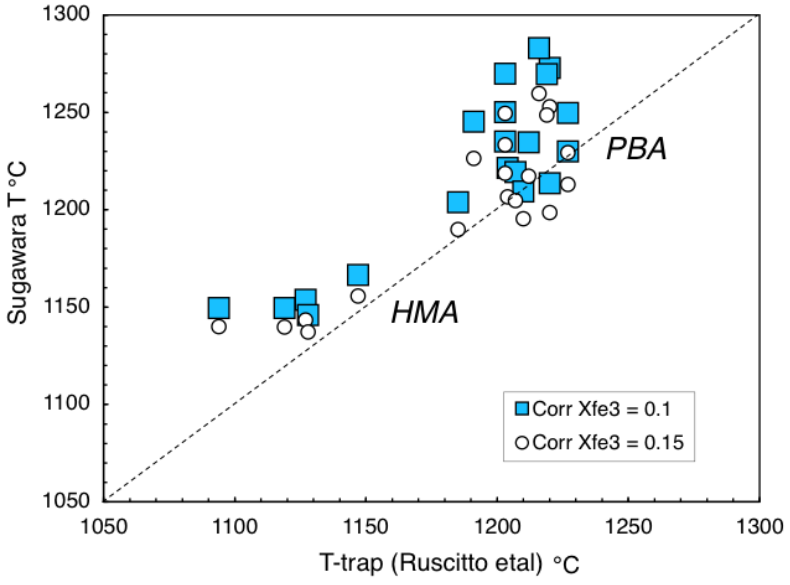

SUPPLEMENTAL FIGURE A4. Comparison of temperature estimates for trapping of melt inclusions (MIs) in HMA olivines. Our temperature estimates are based on the Sugawara (2000) olivine-melt thermometer assuming two values of X-fe3. These agree well with estimates of Ruscitto et al. (2011) for MI entrapment conditions.

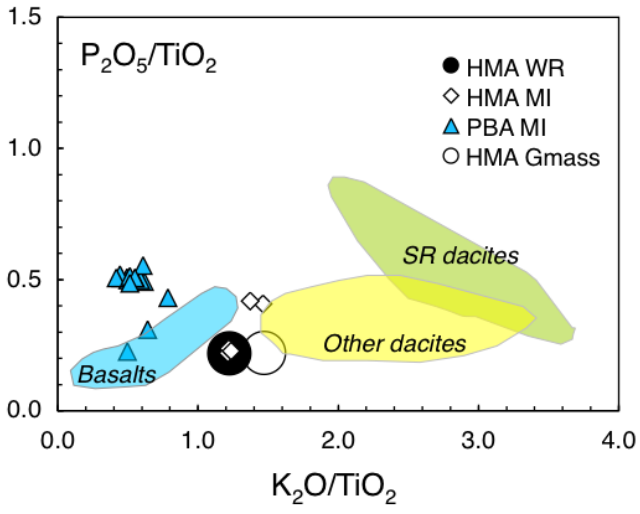

SUPPLEMENTAL FIGURE A5. P_2O_5/TiO_2 vs. K_2O/TiO_2 ratios in Shasta lavas and melt inclusions (MIs). Plotted points are based on data from Table 6. Fields for Shasta basalts and dacites are based on data from Baker et al. (1994), Grove et al. (2002, 2005) and this paper; note that dacites of Sargents Ridge age are distinct from most other Shasta dacites.

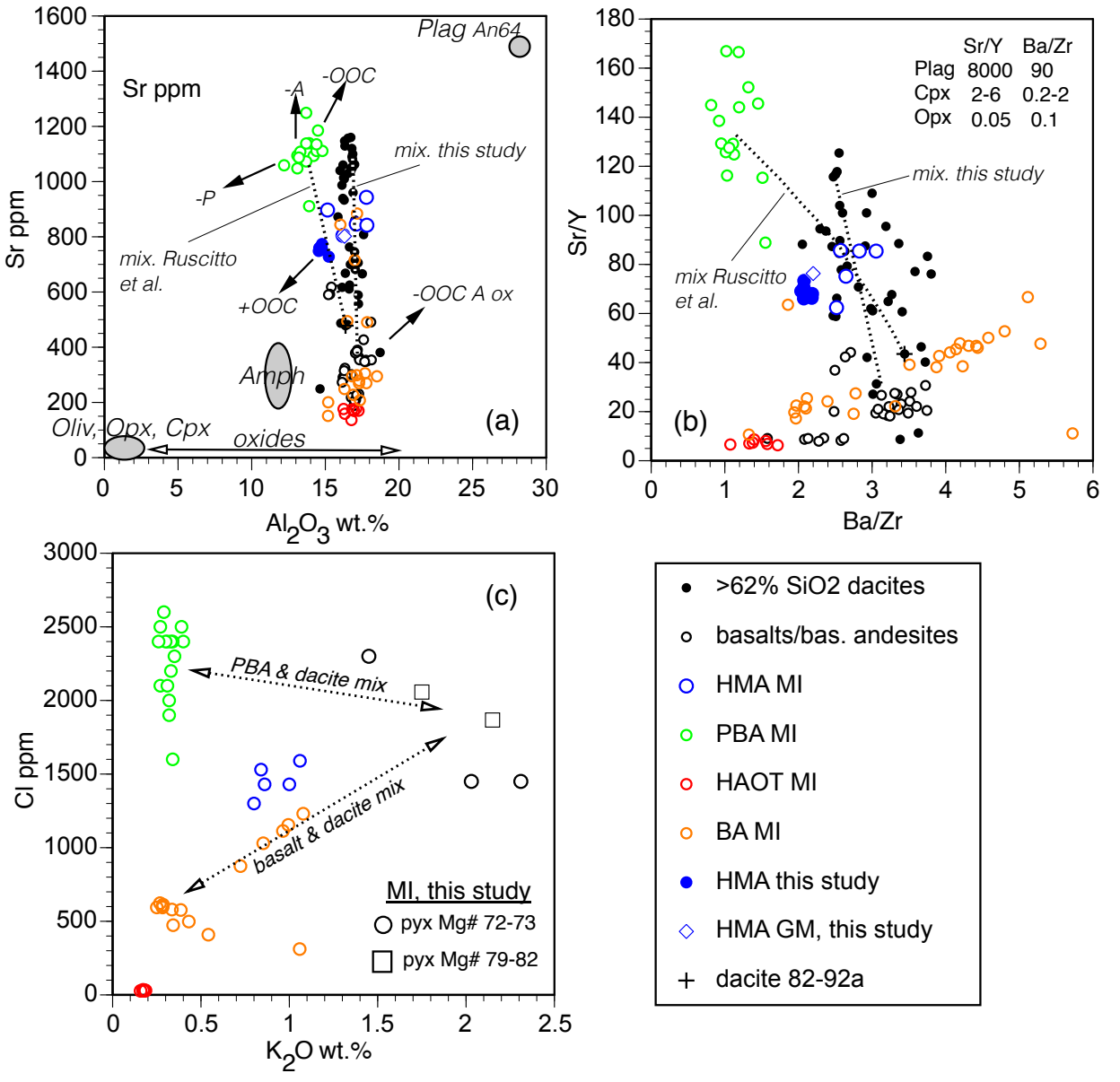

SUPPLEMENTAL FIGURE A6. Comparison of compositions of melt inclusions (MIs) with Shasta area lavas. These diagrams highlight the exotic nature of the PBA-type inclusions. Dashed lines in (a) and (b) contrast mixing between PBA and Shasta dacite 82-92a as proposed by Ruscitto et al. (2011) versus mixing between high-Sr dacite and calcalkalic basalt as proposed in the present study. Arrows in (a) indicate schematically expected composition shifts due to removal (-) or addition (+) of minerals; P = plagioclase, A= amphibole, OOC=olivine, opx, and cpx, ox. = oxides. Sources of data: bulk rock data for dacites, andesites and basalts: Baker et al. (1994), Grove et al. (2005); HMA bulk rock and groundmass: this study (Table 2); basaltic andesite (BA) and high-alumina olivine tholeiite (HAOT) MIs: Le Voyer et al. (2010); HMA and PBA MIs: Ruscitto et al. (2011). Mineral compositions are based on our LA-ICPMS data for minerals except for amphibole and oxides which are estimated. In (c), 'pyx Mg#' denotes Mg# of clinopyroxene hosts for dacitic MIs (cf. Tables 2 and A2).

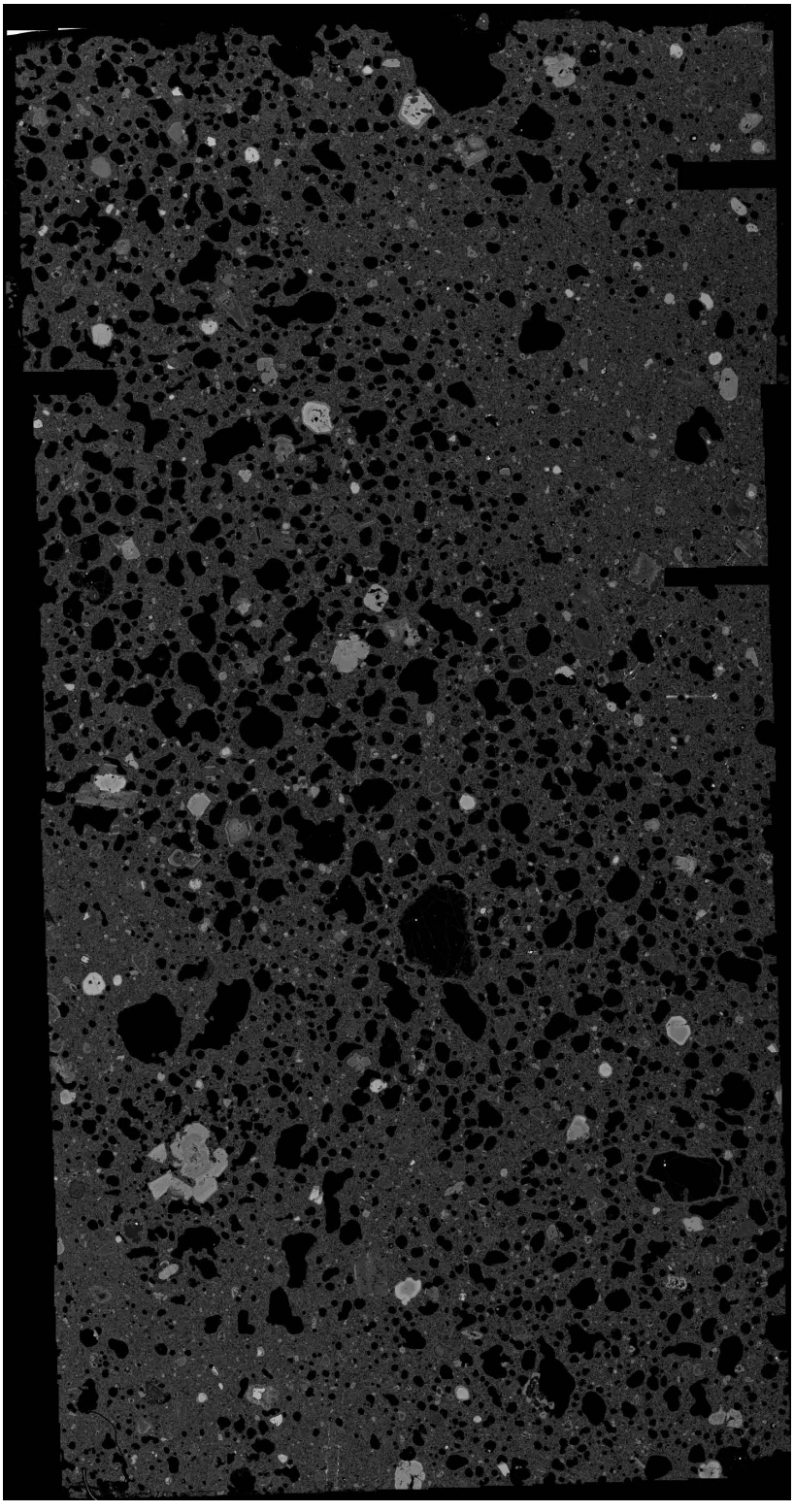

Supplemental Figure A7. Large area BSE map of thin section MS1604b. This 56225x29580 pixel map was created from 550 individual images acquired in a rectangular array with Oxford INCA software. Images were stitched in the Matlab programming language using a cross-correlation algorithm for precise image alignment (Hugo et al, 2015).